Finite Element Analysis and The Modeling of Tires

D. V. Wallerstein and G. A. Dilley
The MacNeal-Schwendler Corporation

ABSTRACT

An area of continuing interest within the tire industry is the modeling and analysis of tires subject to general loading conditions. This paper will focus on the use of MSC/NASTRAN to model a typical radial tire. In addition to discussing this particular tire model and the results obtained from the analysis, some brief remarks will be given on the general topic of tire modeling and analysis.

FINITE ELEMENT ANALYSIS AND THE MODELING OF TIRES

INTRODUCTION

Although the modeling and analysis of tires has been an area of continuing interest within the tire industry, considerable work remains before an adequate general tire model can be constructed. By adequate, it is implied that the model will reliably predict both the global and local response of the tire under a large variety of general loading conditions. Over the past two decades a number of models have been proposed which have inherent limitations. The simplest of these models consists of joining two concentric elastic rings by numerous springs and dampers. Major problems exist with this model in that determining the equivalent material properties is difficult and the model can predict only limited global behavior. Another model type is the two-dimensional axisymmetric finite element model. These models are incapable of representing the anisotropy of the tire in the circumferential direction and are restricted to axisymmetric loading conditions. This paper focuses on a third type of model, the three-dimensional shell finite element model constructed from two-dimensional plate elements. In these models the anisotropy of the tire is characterized by using composite plate elements. In addition, the model may be subjected to arbitrary types of loading. For a discussion of several types of models see "Tire Stress and Deformation," by R. A. Ridha and S. K. Clark [1] and NASA CP-2264 [2].

TIRE CONSTRUCTION AND COMPONENTS

The three primary types of tires currently in production are bias, belted-bias and radial. These tires are composed of layers (plies) of parallel cords (nylon cords or steel wire belts) embedded in rubber. When these plies together with the other layers of rubber are vulcanized under pressure they become an integrated structural unit which can endure severe stresses and deformations (see Figure 1). It is the variation of cord angles in the plies and the use of steel belts which has led to the categorization of tires into three types. Bias tires generally have either two or four body plies with the cord directions essentially symmetric to the centerline of the tread, at rather large angles with the centerline, and anchored around the

bead (see Figure 2). Belted-bias tires have the basic ply body of bias tires plus two or more cord belts. These belts are oriented in a circumferential direction to restrict the inflated tire configuration (see Figure 3). Radial tires are also belted but have all the body cords oriented perpendicular to the tread centerline (see Figure 4). For more information on the construction and design of tires see "Structure of the Pneumatic Tire", by V. E. Gough [1] and Davisson [3].

A TYPICAL TIRE MODELED WITH MSC/NASTRAN

The objective of the present study was simply to demonstrate the capacity for predicting tire behavior with the existing finite element technology. Using linear elastic material properties and the layered composite plate element, a model was constructed to predict axle load and qualitatively determine the response due to lateral movement of the tread/ground interface.

The finite element model prepared for the study represents half of a full three-dimensional tire. Figure 1 shows a typical cross-section of a radial tire. As the figure shows, there may be as many as eight major components present in a radial tire. The radial tire modeled in the current study contained twelve major components. The finite element model consisted of 616 physical grid points with 2094 degrees of freedom used in the analysis. Figure 5 shows the distribution of grid points used to model each cross-section. Figure 6 shows the number of sectors used in the model. In the footprint region there were five sectors each spanning 3° of arc, while elsewhere each sector spanned 15° of arc. The grid spacing in the footprint area was chosen so as to obtain an adequate definition of the footprint. Elsewhere, the grid spacing was selected in order to maintain an aspect ratio less than 5 to 1 for the QUAD4 elements. The following elements were used in the model.

416 QUAD4 anisotropic plate elements to model the basic tire including the individual component plies (see Figure 7 for a typical ply lay-up).

32 BAR elements to model the tire bead.

54 GAP elements to represent the tread and tread/ground contact.

34 Torsion spring elements to model the torsional stiffness of the rubber in the bead region.

The GAP elements used in the current model were included for several purposes. First, they provided a means for determining the footprint area. Second, they provided a way of applying friction resistance to lateral sliding of the tire. And finally, the GAP elements were used to input the tread stiffness. Future studies should determine if better methods can be formulated for incorporating the tread stiffness in shell models.

A cylindrical coordinate system, centered on the axle centerline in the plane of the tread centerline, was used to define the grid point locations for the tire model. This coordinate system is depicted in Figure 8. Figures 9 and 10, which were generated using MSC/GRASP, show several views of the undeformed model.

The analysis treated the tire as being geometrically and materially (GAP elements) nonlinear with the following loading conditions applied:

1) The bead grids (XX35 and XX36) were forced radially outward 0.04 inches and the grids at the tire/rim interface (XX33, XX34, XX35 and XX36) were forced laterally outward 0.06 inches to represent the preload resulting from mounting the tire on the rim.

2) The tire with the bead preload was inflated to 35 psi.

3) Under conditions 1 and 2, the tire was given a vertical displacement of 1.2 inches in the footprint area.

4) With all the above loading conditions in effect, the tread was then moved laterally 1.0 inches.

Loading conditions 3 and 4 were applied through a single node (99000) which was connected via a rigid body element (RBE2) to all of the ground nodes (X01 to X09).

RESULTS

Figure 11 gives a plot of the tire deflection versus axle load. In each of the analyses which have been performed thus far at MSC, the axle loads were computed to within 15% of the loads obtained experimentally. In particular, the most recent model obtained an axle load which was well within 5% of the experimentally determined load. This indicates that the models provide a reasonable measure of the tire stiffness due to axle load.

Figures 12-15 show MSC/GRASP generated plots (not true scale) of the deformed tire for each of the four load cases used in this study. Figure 12 gives an exaggerated view of the tire displacements resulting from the enforced bead displacements. Figure 13 represents the displacements resulting from the 35 psi inflation pressure. Figure 14 shows the displacements resulting from the 1.2 inch vertical displacement imposed in the footprint region. In each of these figures a front view and the outline of the displacement pattern in the yz-plane is given. In Figure 15 three views of the deformed tire are shown which result when the 1.0 inch lateral sliding is enforced. Figure 16 shows the cross-section deformation (true scale) at the footprint ($\theta = 0$) for each of the four load cases. Figure 17 shows the deformed tire (under all four load conditions) overlayed with the undeformed tire.

CONCLUSIONS

Radial tires are not symmetric about the tread centerline. It is, however, possible to model tires using segment models and half tire models. The belt pattern is the main concern when deciding whether to use a segment model or a full model. Consider Figure 18 which shows a typical layer of belt. Figure 18a shows how the belt crosses the tread centerline in a physical tire, while Figure 18b shows the implied belt pattern when a half model with symmetry constraints is used. If the belts are included with $\pm\theta$ layers and if the layers are not separated by a significant amount of interply rubber, then a half tire model may adequately characterize the "average" ply behavior.

Segment models whereby only a few degrees are modeled are of course very useful in initial model checkout. Also with elaborate MPC's to enforce the axisymmetric conditions, they can be used to predict tire inflation with reasonable accuracy. If the belt and body ply lay-up is "choppy", that is, some belts are oriented at odd angles to all other belts or some of the belts extend further into the shoulder area than other belts, then a full tire model should be considered.

The tire is essentially a toroidal shell structure. Mesh size changes may cause numerical inaccuracies in the calculation of pressure loads. These inaccuracies may in turn cause a circumferential load to be produced at the boundary between the meshes of differing size. This load tends to impose a rigid body motion on the model. This effect may be significant for a model with a small overall deflection. In addition to mesh size changes, care must be exercised in defining the orientation of the material axes. It is best to define the material x-axis as being parallel to the tread centerline. This will prevent additional numerical inaccuracies due to rotations of the principal material axes from appearing in the model.

The tire can best be represented as a thick-walled anisotropic shell structure. The authors feel that more exhaustive testing needs to be performed to substantiate the use of shell elements before investigating the use of solid elements for tire modeling. Three-dimensional elements are very

expensive to use and it is not clear in our minds that they would improve the model description. The tire load carrying capability is essentially similar to thick-walled shells and much fruitful research should be carried out in studying model sensitivity to such items as load paths and variation in ply lay-up.

The authors think that they have shown that finite element modeling of tires is feasible and worthwhile. The authors also feel that meaningful finite element modeling of tires offers the tire analyst an interesting and challenging application of the finite element method.

REFERENCES

1. Clark, S. K. (ed.); "Mechanics of Pneumatic Tires;" U. S. Department of Transportation; DOT HS-805-952; August 1981.

2. Tanner, J. A. (ed.); "Tire Modeling;" Proceedings of a Workshop held at Langley Research Center, September 7-9, 1982; NASA Conference Publication No. 2264, 1983.

3. Davisson, J. A.; "Design and Application of Commercial Type Tires;" SAE Paper No. 690001.

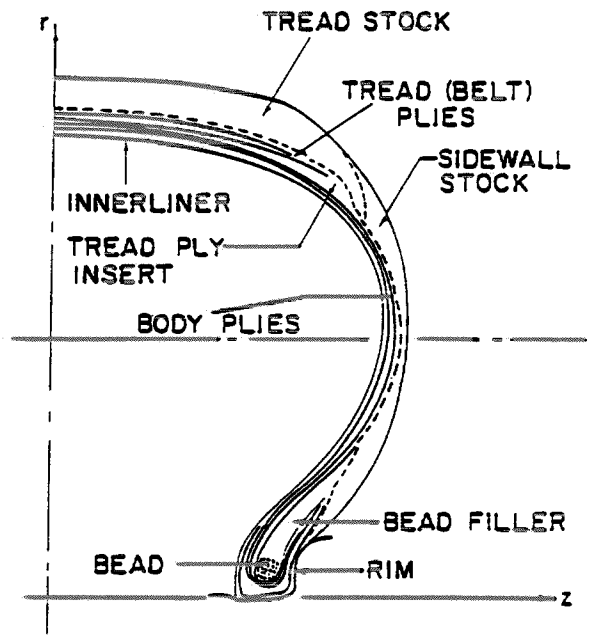

Figure 1. Cross-section of a Belted Tire.
Reference: Ridha and Clark [1]

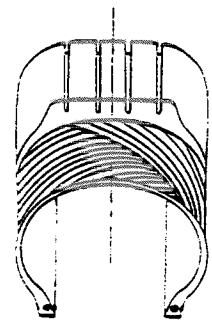

Figure 2.
Cord Pattern in a Bias Tire

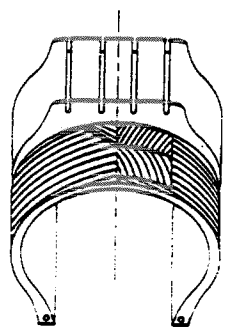

Figure 3.
Cord Pattern in a Belted-Bias Tire

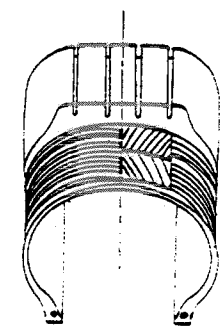

Figure 4.
Cord Pattern in a Radial Tire

REFERENCE: KIDHA AND CLARK [1]

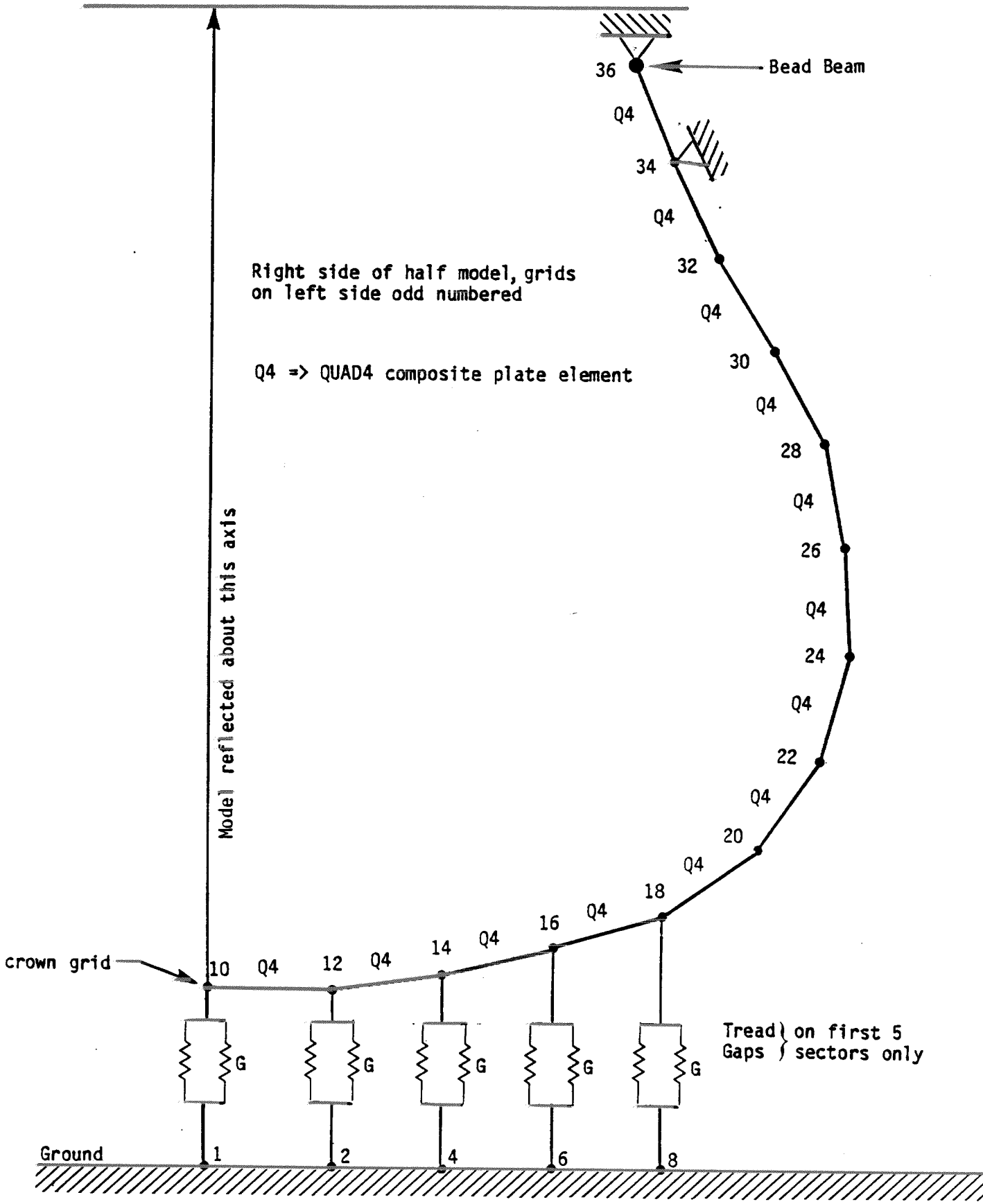
Bead Beam
36
Q4
34
Q4
32
Q4
30
Q4
28
Q4
26
Q4
24
Q4
22
Q4
20
Q4
18
Q4
16
Q4
14
Q4
12
Q4
10
Right side of half model, grids on left side odd numbered
Q4 => QUAD4 composite plate element
Model reflected about this axis
crown grid
G
G
G
G
G
Tread on first 5 Gaps sectors only
Ground
1
2
4
6
8

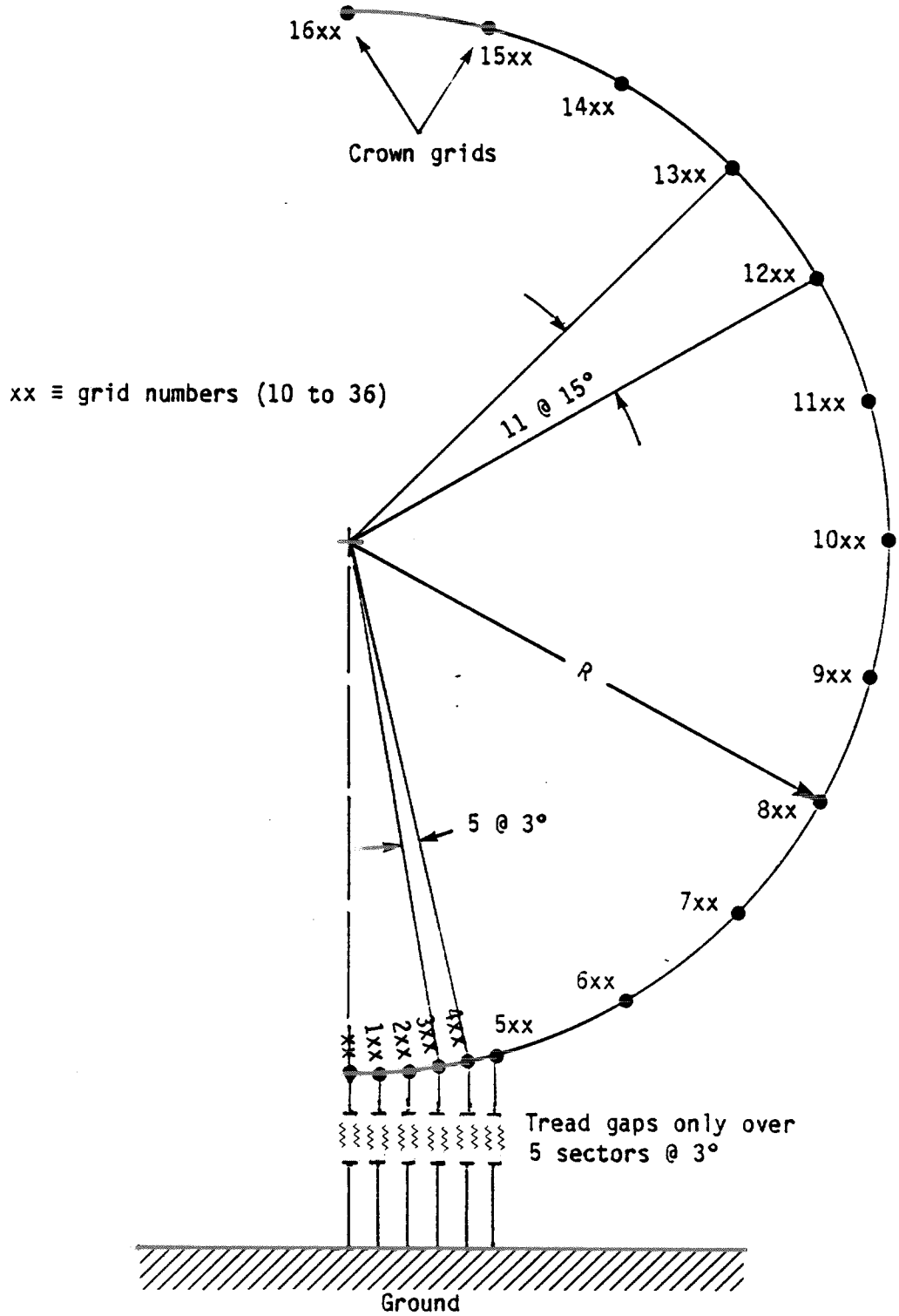

Figure 6. Representative Number of Sectors for Half Tire Model.

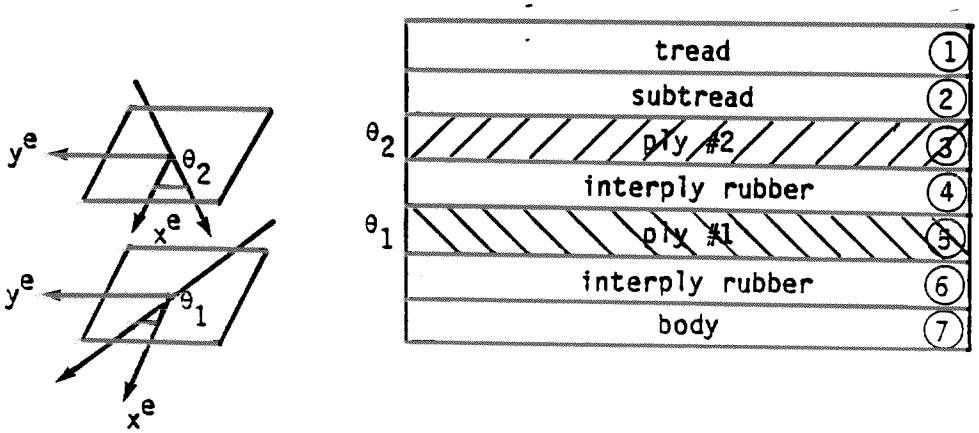

Figure 7. Typical Ply Lay-up for a Radial Tire.

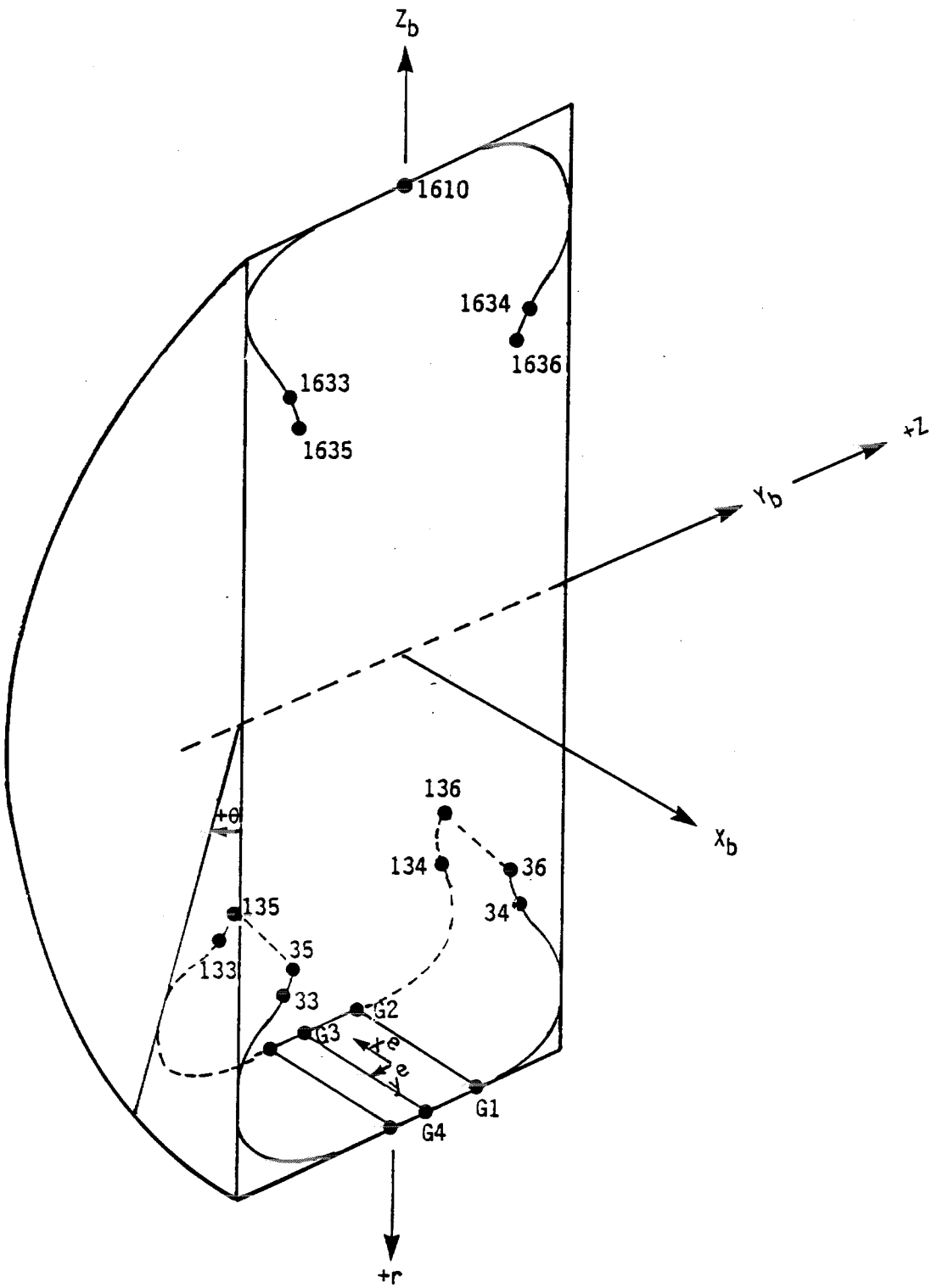

Figure 8. Model Coordinate Systems.

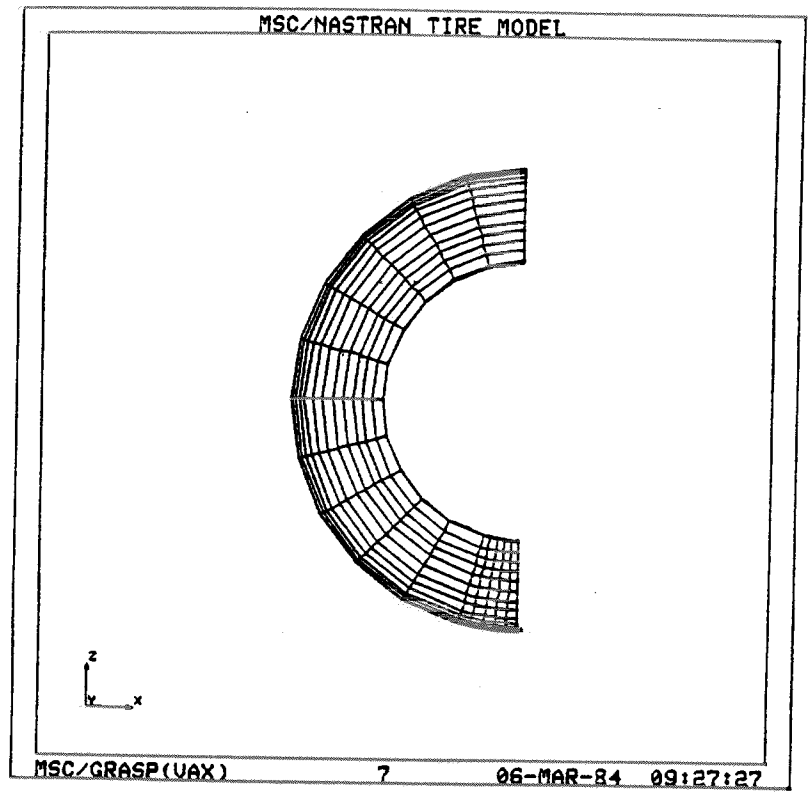

Figure 9a. Tire Model - Side View

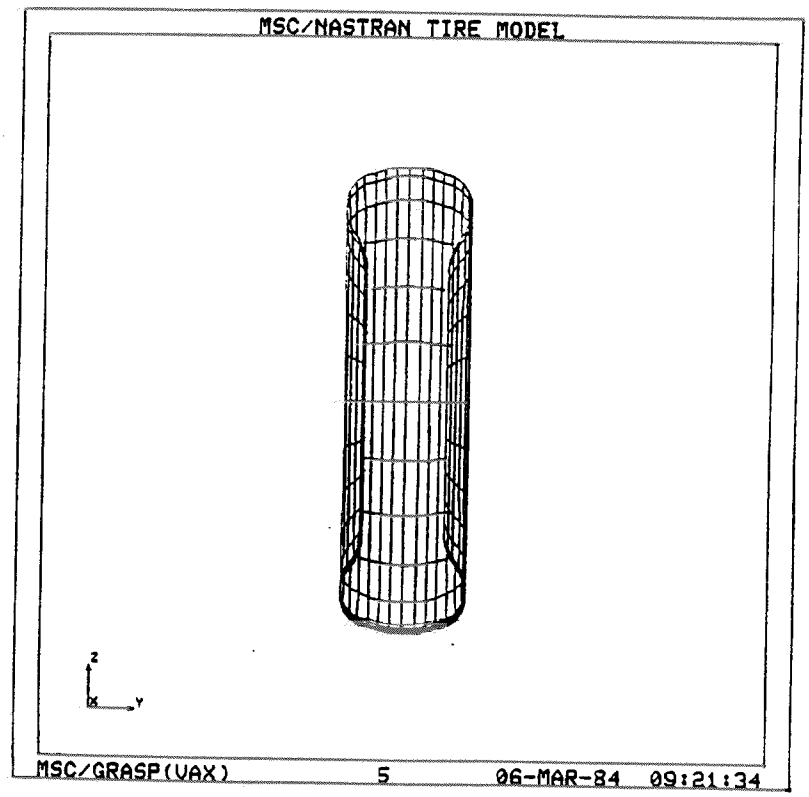

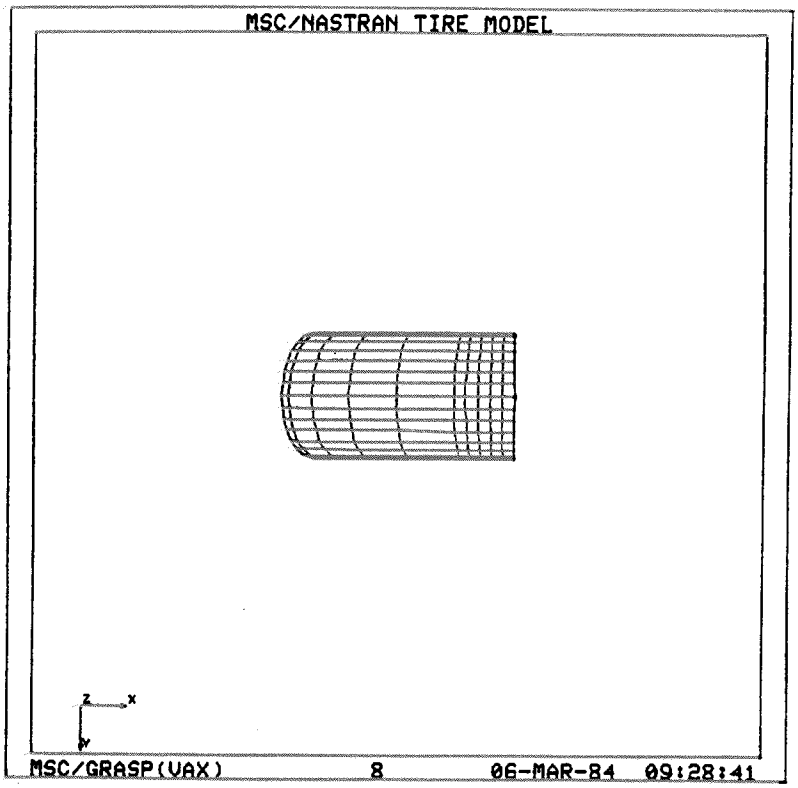

Figure 9c. Tire Model - Bottom View

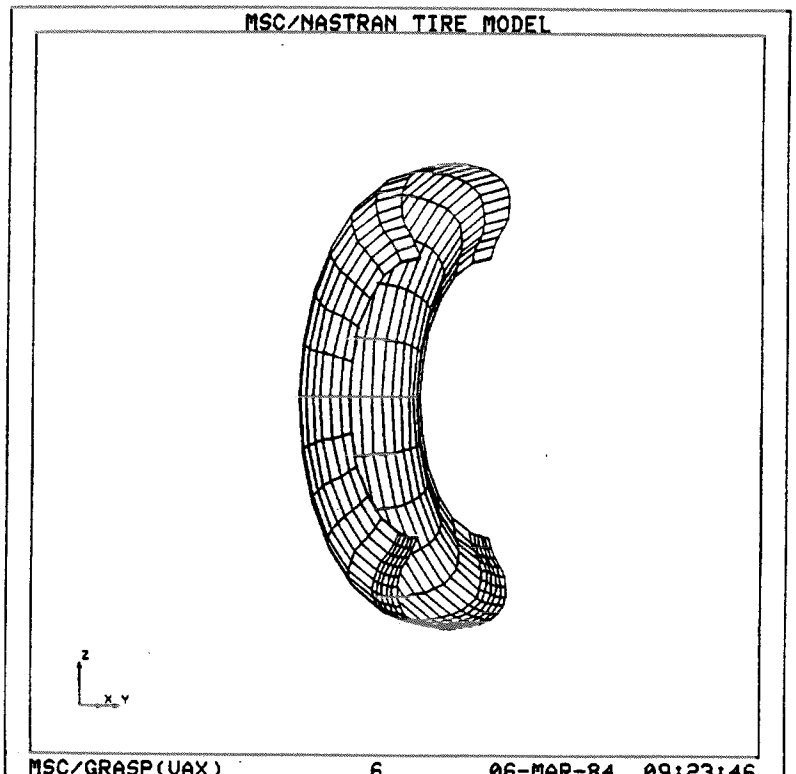

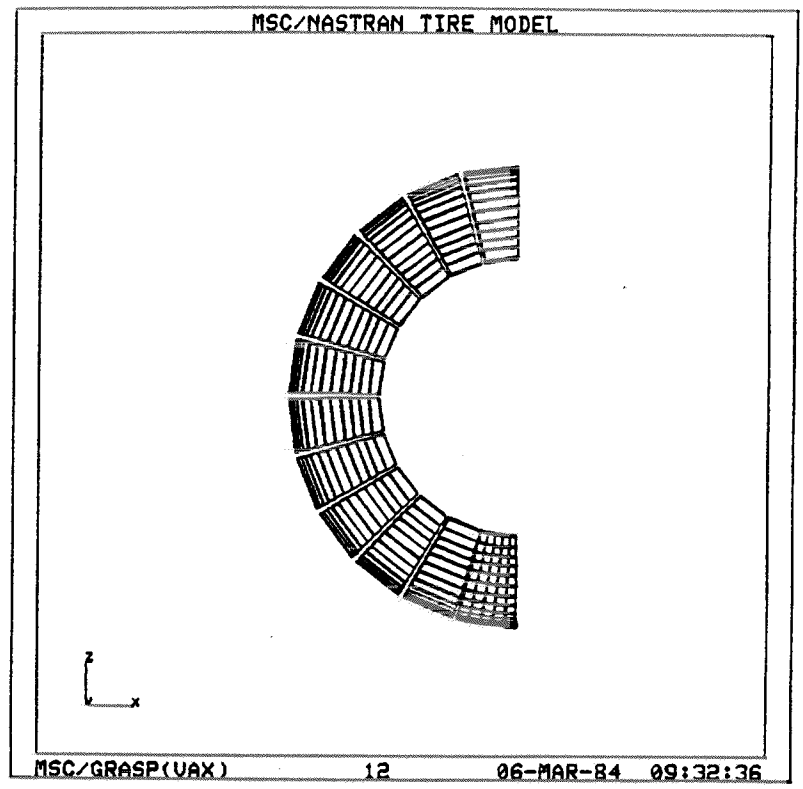

Figure 10a. Tire Model - Side View, Element Shrink

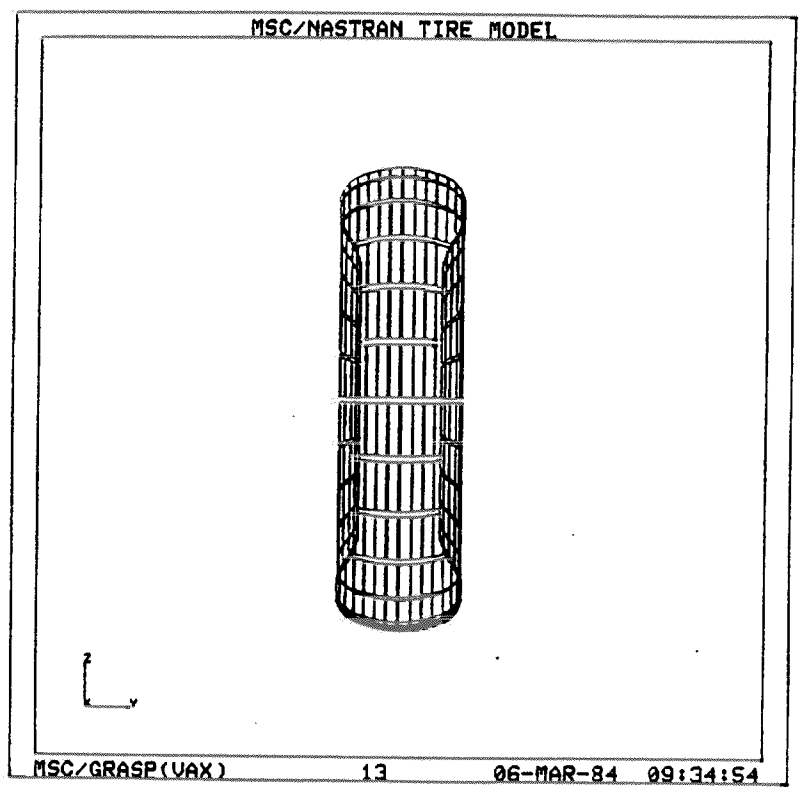

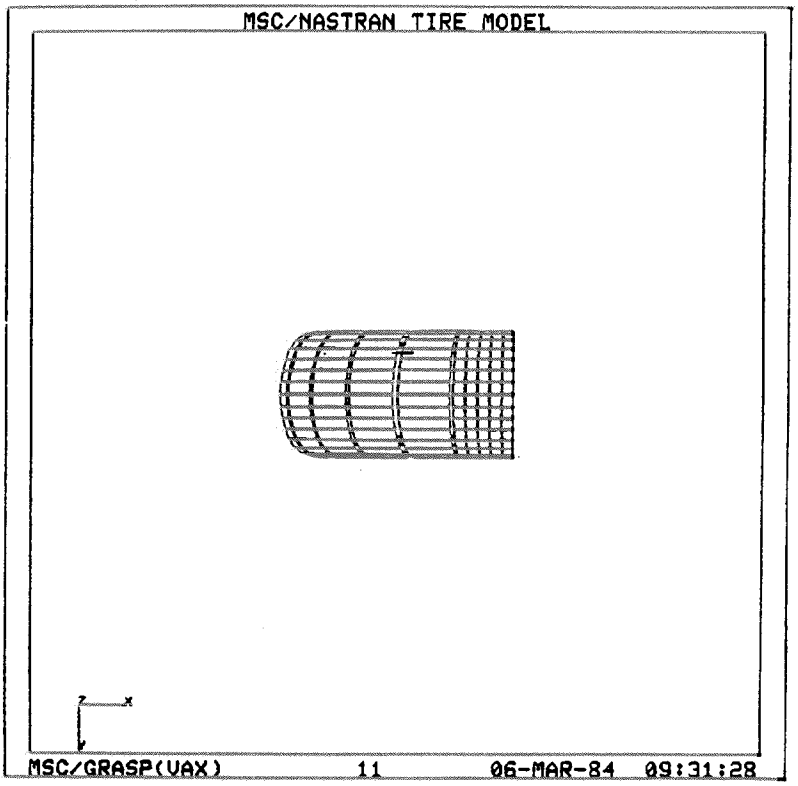

Figure 10c. Tire Model - Bottom View, Element Shrink

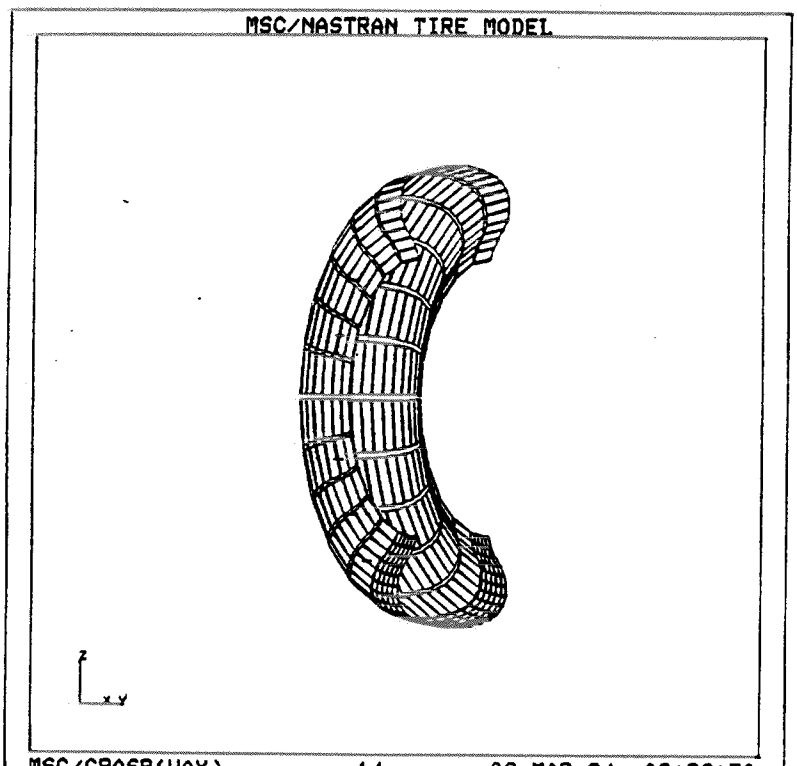

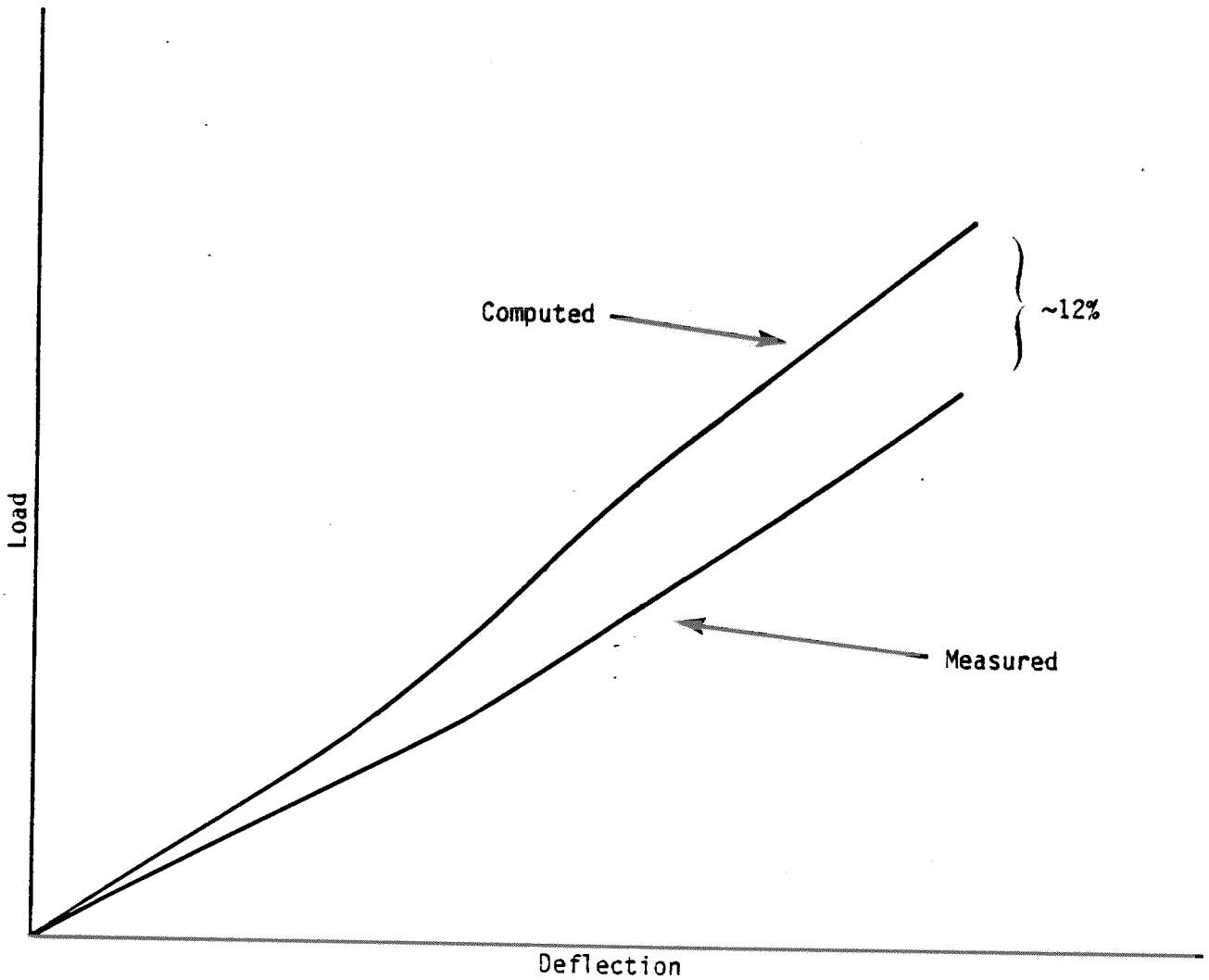

Figure 11. Axle Load Versus Deflection.

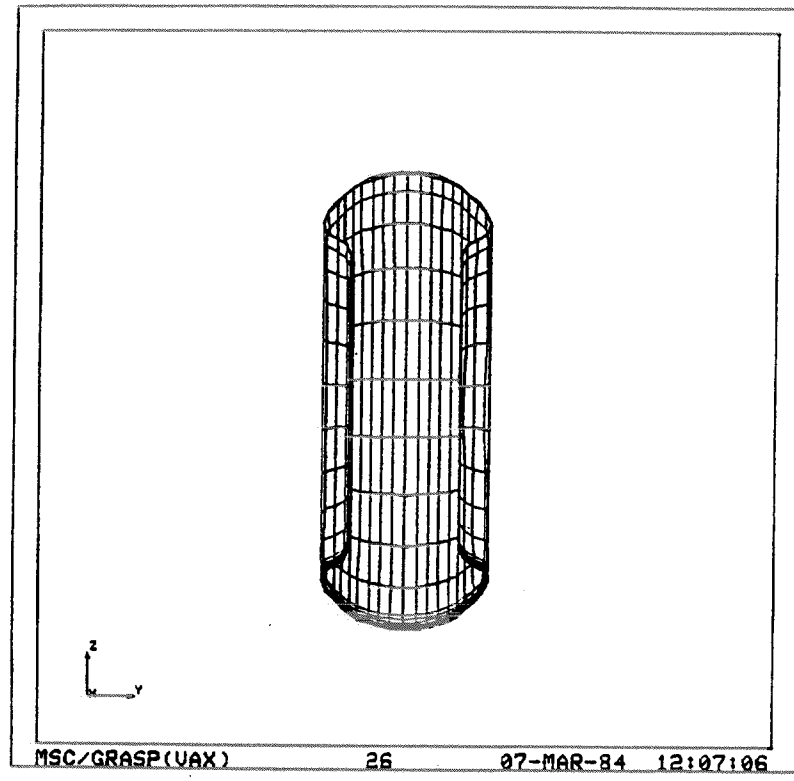

Figure 12a. Bead Load - Front View

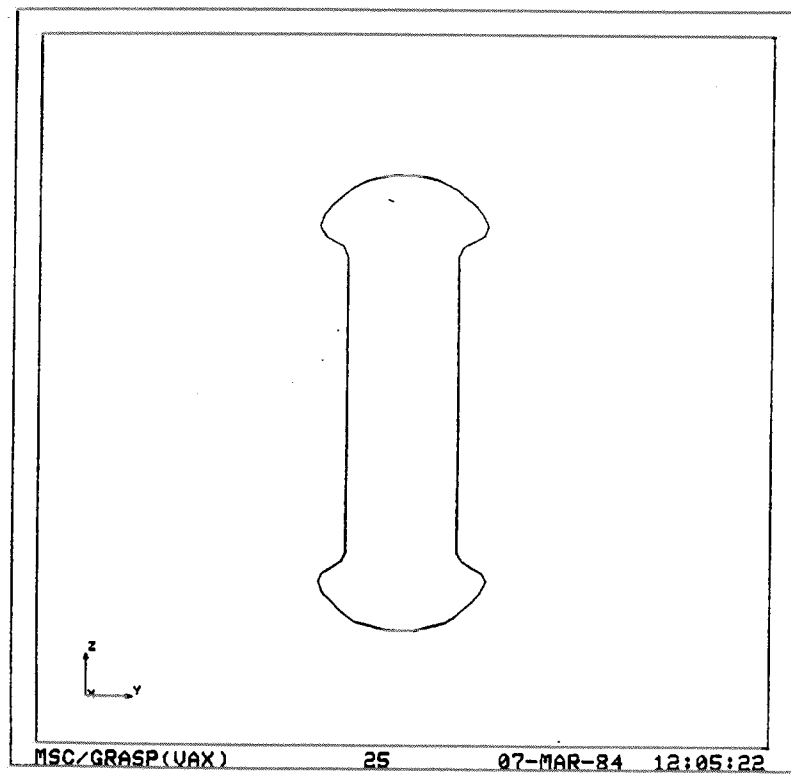

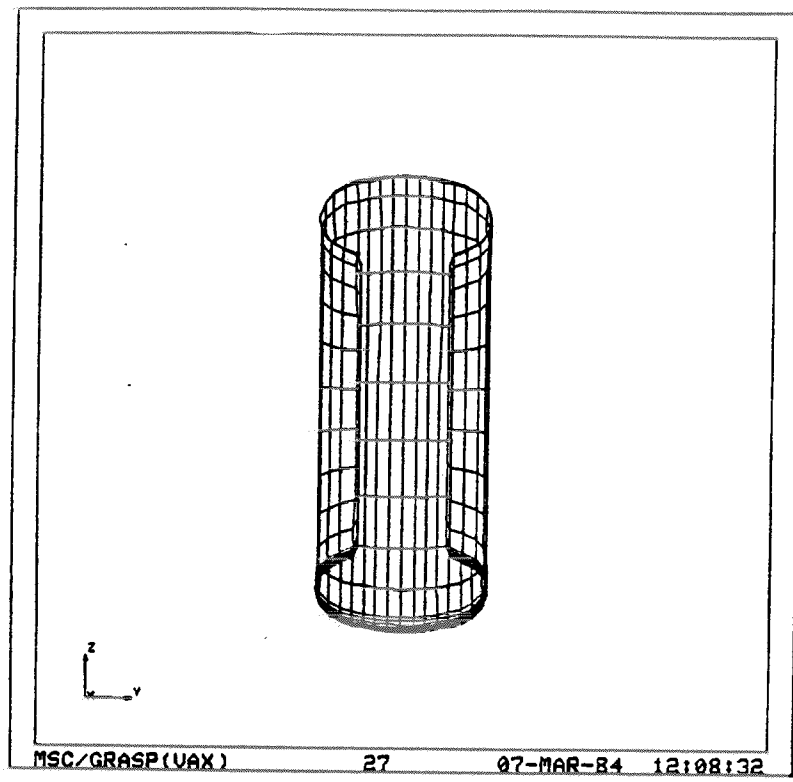

Figure 13a. Tire Inflation - Front View

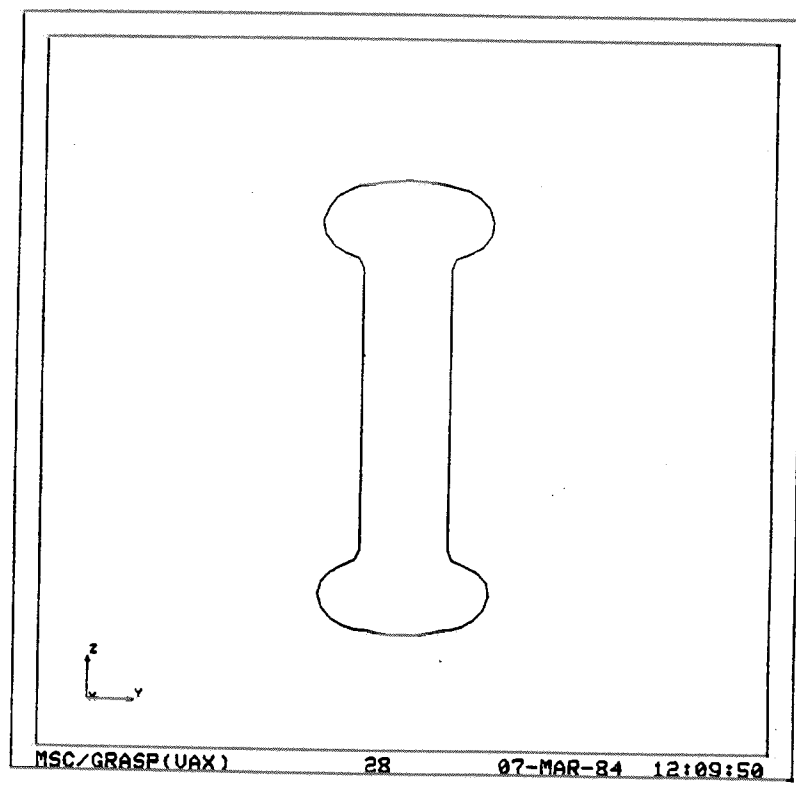

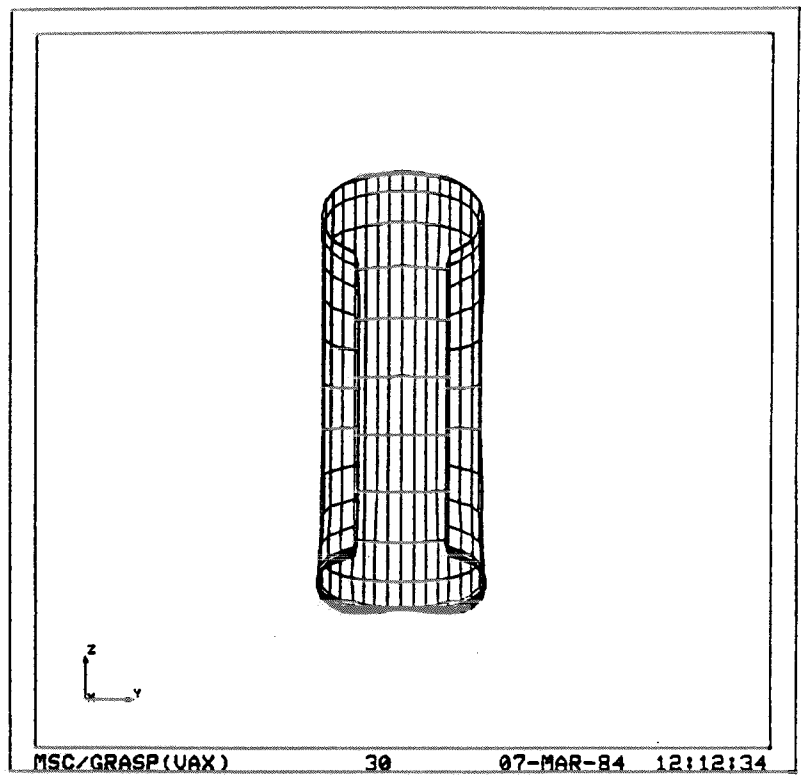

Figure 14a. Footprint - Front View

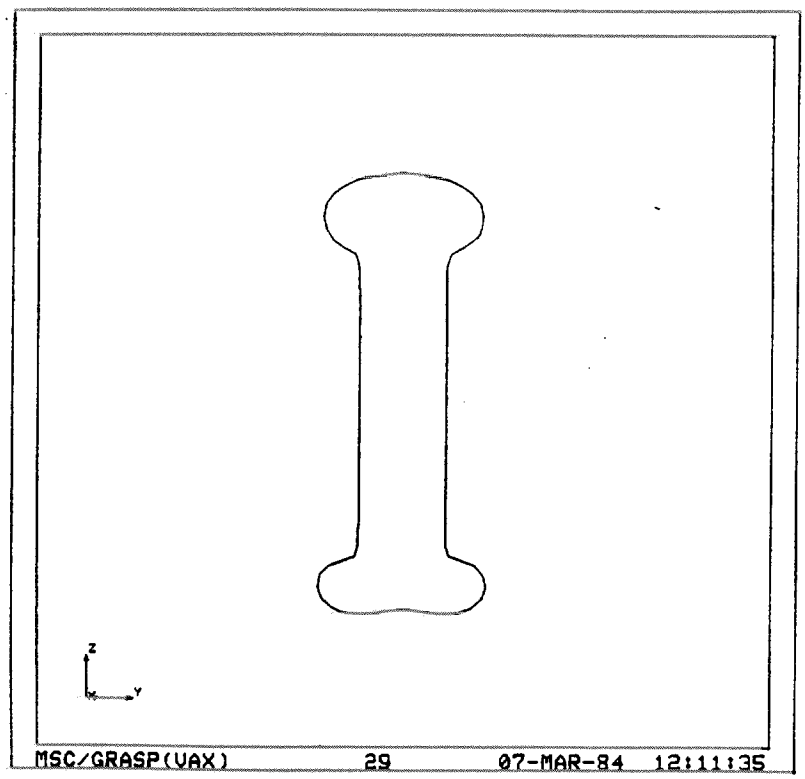

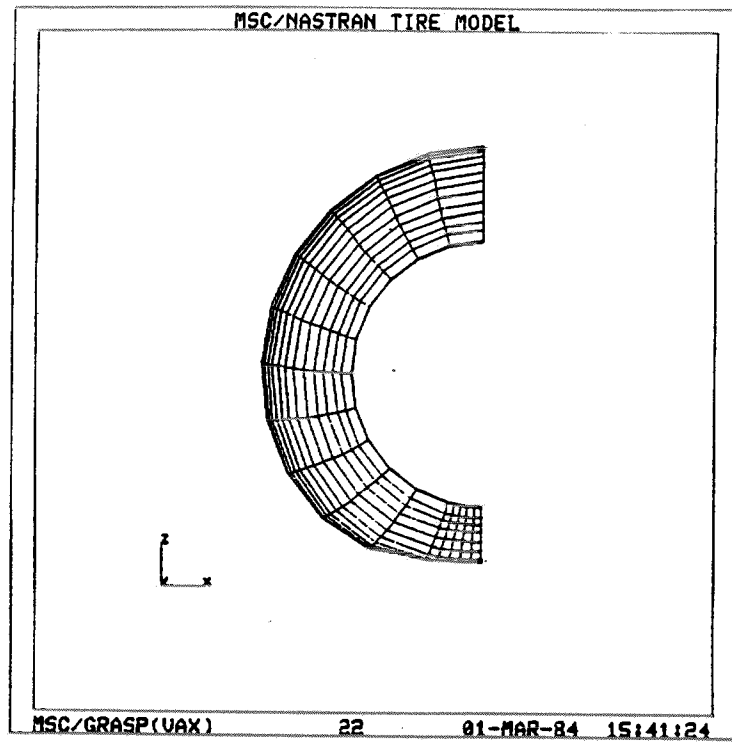

Figure 15a. Lateral Sliding - Side View

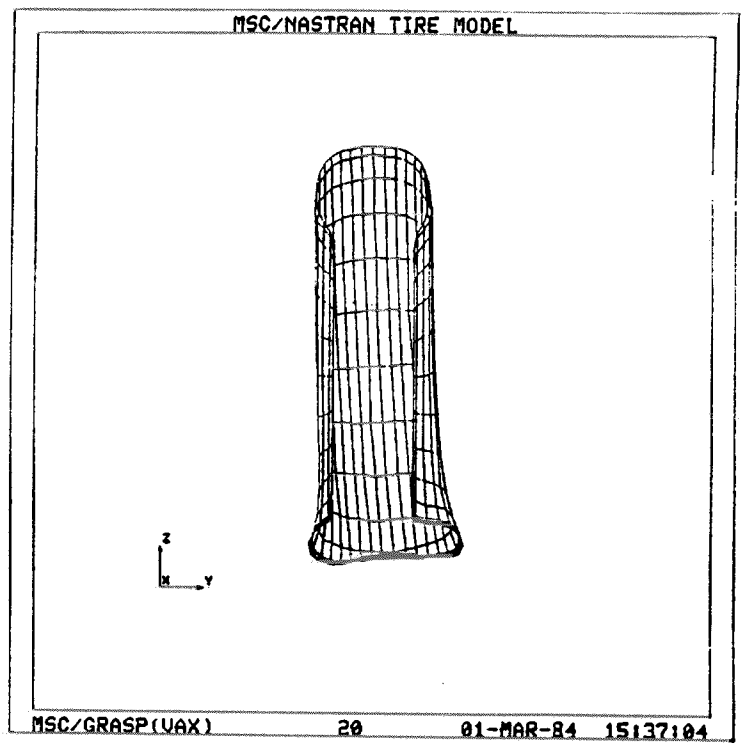

Figure 15b. Lateral Sliding - Front View

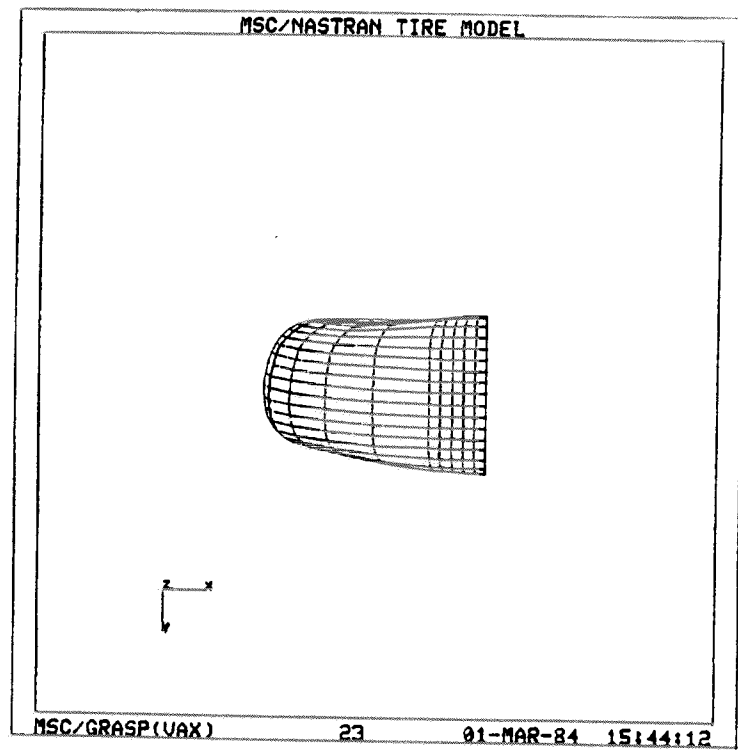

Figure 15c. Lateral Sliding - Bottom View

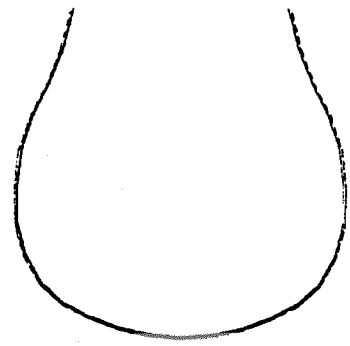

Figure 16a. Bead Load

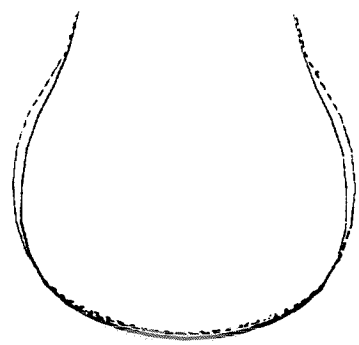

Figure 16b. Tire Inflation

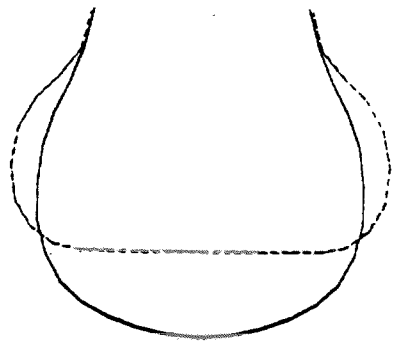

Figure 16c. Footprint

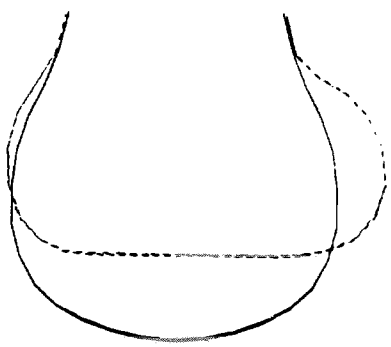

Figure 16d. Lateral Sliding

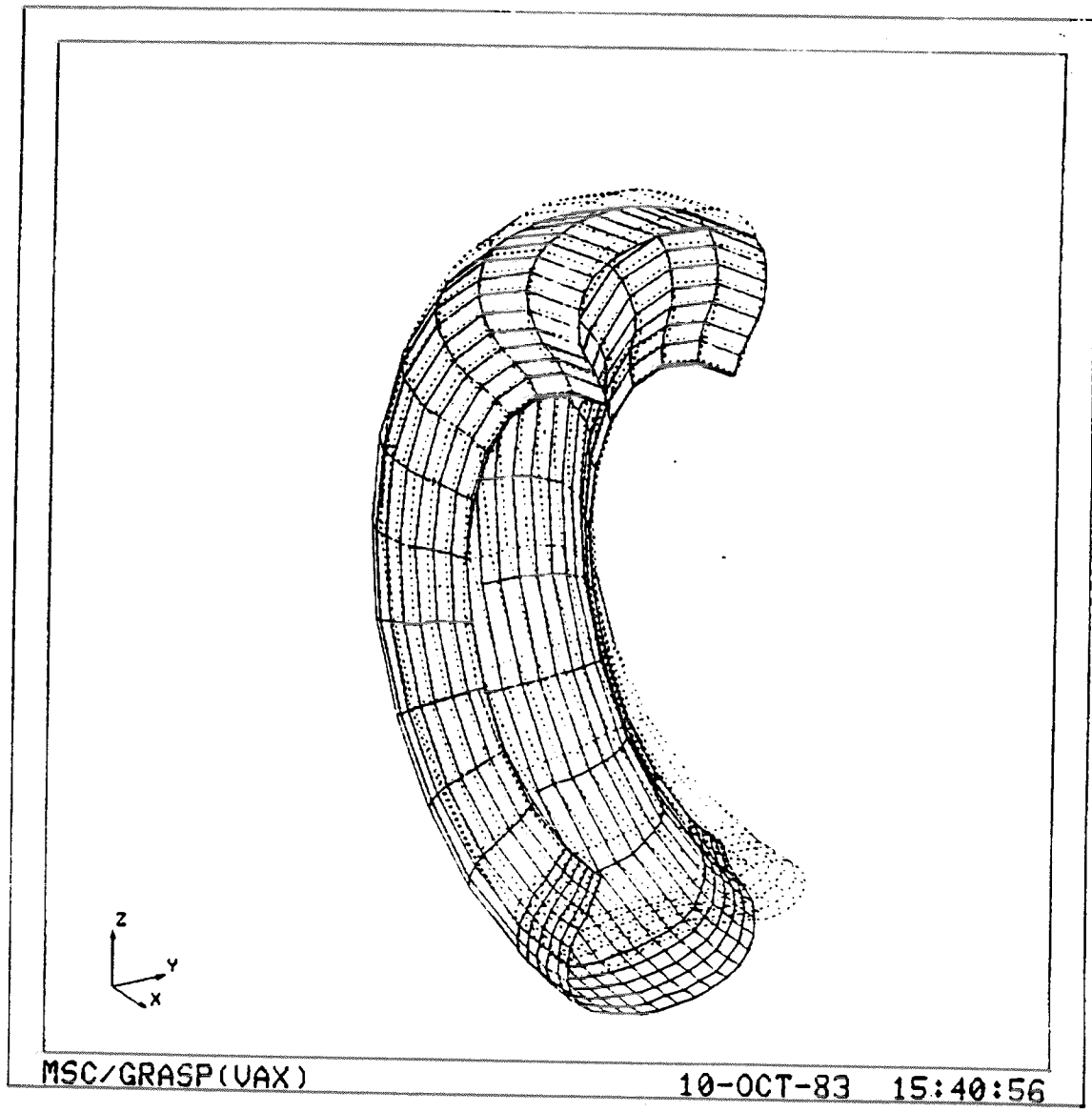

Figure 17. Composite View of Undeformed and Deformed Tires

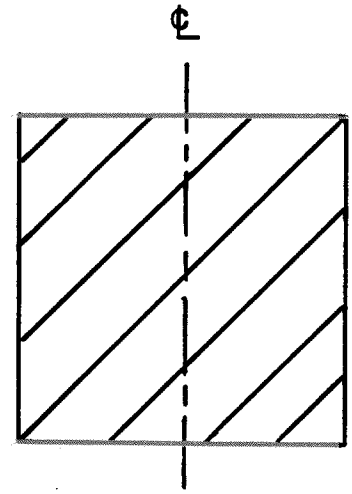

Figure 18a. Belt Layer-Actual.

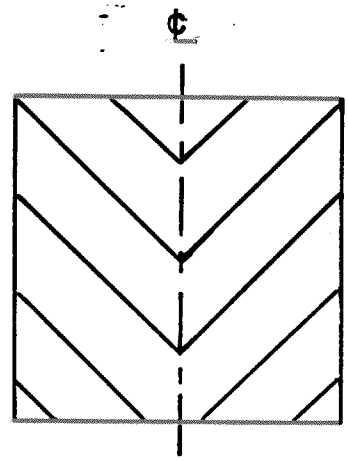

Figure 18b. Belt Layer-Idealization.